Chengdu 2019 Symposium

https://www.cigre.org/

0156

Verifying potential impacts of microgrids by its modeling in power distribution system simulators

H. I. ETO, E. C. VEIGA, M. G. R. LEANDRO, V. A. SILVA, F. J. LACHOVICZ, A. R. AOKI
Federal University of Parana, Federal University of Parana, Federal University of Parana, Federal University of Parana, LACTEC, Federal University of Parana
Brazil

SUMMARY

The growing interest in microgrid research has motivated the use of distribution system simulators that support modeling of three-phase unbalanced load systems, distributed generation units, energy storage and controllable loads, within a microgrid. However, despite the significant amount of published works on this subject, few papers have presented in detail the modeling of each element considered in this type of simulation. Thus, this paper, in addition to offering such information, also presents results of simulations that aid in the evaluation of the impacts of a microgrid and its elements on the distribution system. In a scenario with three penetration levels of photovoltaic generation, energy storage, some profiles of load curves, each component was gradually inserted in the model to allow the evaluation of its impact on the distribution system. The microgrid islanding condition was also modeled and made it possible to verify the autonomy of the microgrid evaluated. Simulation results show the effect of voltage level raising on the microgrid busbar, which, although directly proportional to the penetration level of photovoltaic generation, can be attenuated with the insertion of the storage system. The results also show a reverse flow in the distribution transformer that connects the microgrid to the main grid due to the penetration of the photovoltaic generation. Both simulators of distribution systems used in this work, GridLab-D and OpenDSS, presented adequate results for the calculation of unbalanced three-phase power flow. Moreover, GridLab-D presented suitable results for the simulation of microgrids, where there is the possibility of islanding.

KEYWORDS

Microgrid - Distribution system simulator - Microgrid modeling - Unbalanced power flow

itiroeto@gmail.com

1. INTRODUCTION

The permanent need to make the power system increasingly sustainable, resilient, and integrated has created several challenges for the scientific community. Particularly in the distribution system area, the solutions pointed out in recent researches to overcome such challenges have usually encompassed topics such as distributed generation (DG), energy storage system (ESS), demand response, microgrid (MG), and virtual power plants among others. However, the potential impacts which these technologies can cause on current distribution systems have been a concern for operators, maintainers, and designers of that. Invisibility to the system operator, the possibility of reverse power flow, the impact on conventional protection schemes, as well as the increase in local voltage levels, are some examples. Current distribution systems have not been designed or even prepared to absorb these technologies without requiring some adaptations in processes, equipment, control, supervision, etc.

Several works regarding this issue have shown that solutions to overcome these new challenges require a software modeling of current power systems with such new technologies to perform tests considering new scenarios, models, and assumptions. Thus, results can be verified adequately despite the inherent complexity of current power distribution systems. For such purposes, platforms of power distribution system simulation have been the primary choice. GridLab-D, OpenDSS, and Matlab Simulink are examples of such simulation platforms. However, few works in this area [1], [2] have presented in detail the modeling of all elements considered in a simulation, as distributed generation, energy storage system, load curve, and disconnect device among others.

Thus, this work aims to evaluate the unbalanced three-phase power flow calculation by two of these computational tools GridLab-D and OpenDSS and describe how each element of the grid was modeled in GridLab-D simulator, considering steady-state modeling. Furthermore, it aims to evaluate the impacts of a microgrid and its components on the distribution system by the simulation.

This paper describes details found in the software modeling of the solar photovoltaic (PV) panels, battery ESS, and the operation in island-mode. The circuit used to modeling de distribution system is the IEEE 13 nodes test feeder. A comparative analysis was carried out between the two software packages, aiming to validate the use of these tools in the simulation of an unbalanced three-phase distribution system. Simulation scenarios were created for three different levels of daily DG penetration. Simulations were done in steps to gradually take into consideration the distributed generation, the battery ESS, and lastly the microgrid islanding effects. Thus, the impacts of the PV penetration, battery ESS, and the autonomy of the microgrid for those three levels of penetration were gradually analyzed.

The impacts on the distribution network identified by the simulation results corroborate with those found in the literature [3]-[5]. Results show a voltage level increase at the low voltage busbar, which is directly proportional to the level of DG penetration. Also, a reverse power flow with more than six hours duration in the distribution transformer was observed in the middle and high level penetration scenarios. On the other hand, results also show that with the insertion of the battery ESS into the system, the increase of local voltage level was lower than one-third of that verified previously. Besides, the storage system avoided the reverse power flow in the distribution transformer in all scenarios. Additionally, it was observed that the battery ESS decreased and flattened the active power flow curve at the distribution transformer.

This paper is structured as follows: Section 2 describes the materials and methods used in simulations. Section 3 presents the results obtained in simulations. A discussion of the results is present in Section 4. Finally, in Section 5, some conclusions and future works are presented.

2. MATERIALS AND METHODS

2.1. Microgrid arrangement within the IEEE 13 nodes model

The IEEE 13 nodes, an unbalanced three-phase test feeder, is the circuit model used in simulations of this paper. In its original form, it consists of 13 bus (nodes), a voltage regulator (RG60) and a distribution transformer (XFXFM1). One bus (634) is in low voltage of distribution (LVD), and the others are in medium voltage of distribution (MVD). This model has nodes with loads of constant power (PQ), constant impedance, and constant current. Although widely used in literature for distribution system simulations, this model does not initially contemplate a microgrid arrangement. Thus, for this work, it was necessary to add in the model, at the LVD busbar, a solar PV, a battery ESS, as well as a disconnect device (between XFXFM1 and 634) to emulate a microgrid in the island-mode operation, as illustrated in Figure 1.

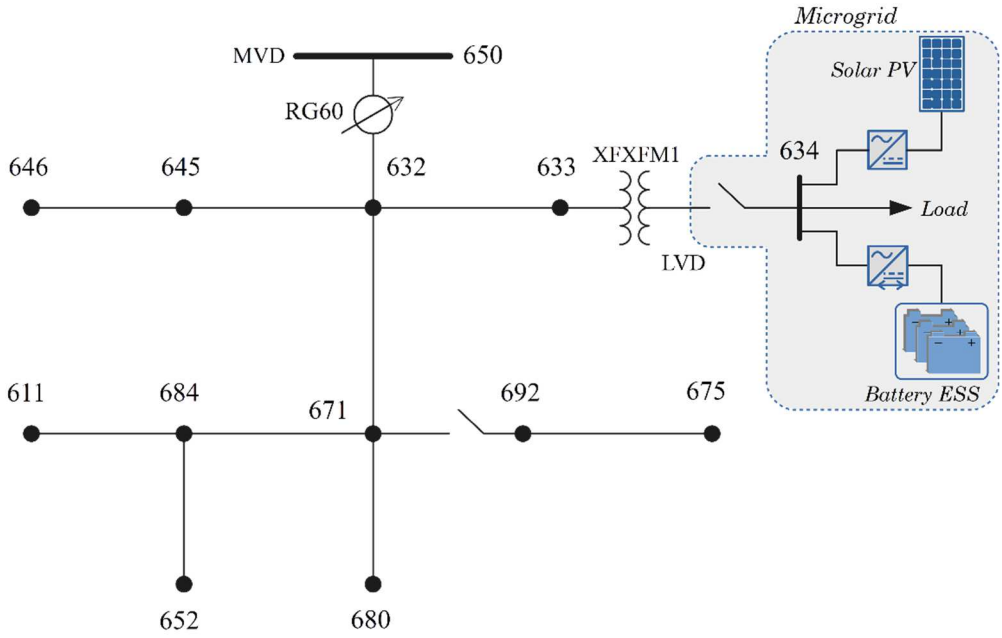

Figure 1: An adaptation of the IEEE 13 node test feeder model, with a microgrid connected at bus 634. Source adapted from [6].

2.2. Simulation Methodology

The distributed energy resources were gradually added to the simulations (in a five-step sequence) to emphasize the impacts on the power distribution system:

- **Step 1 (GridLab-D, OpenDSS):** IEEE 13 nodes system in their original form (as a reference model);
- **Step 2 (GridLab-D):** IEEE 13 nodes system with real load curves and addition of a low voltage of distribution (LVD) network at bus 634;
- **Step 3 (GridLab-D):** step 2 with the addition of PV at bus 634;
- **Step 4 (GridLab-D):** step 3 with the addition of a battery energy storage system at bus 634;
- **Step 5 (GridLab-D):** step 4 with the addition of a disconnect switch to enable the islanding of the LVD microgrid.

Step 1 has both the objective of validating the simulation environment of this work and of validating the results of the three-phase power flow from the simulator through comparison with the reference values from the IEEE 13 nodes model. In this step, two simulators of distribution power systems were used: GridLab-D and OpenDSS. As the former allows the event of opening a switch during the execution time of simulation (to simulate events of disconnection/connection from/to the main grid), and the latter does not, then GridLab-D was adopted as the reference simulator in steps 2 to 5.

In step 2, the original constant loads of the IEEE model, at PQ buses, were replaced by load curves originated from field measurements [7]. In step 3, the PV system was added to bus 634. In step 4, the battery ESS was added to bus 634. Finally, in step 5, a disconnect switch was inserted between bus 634 and the transformer XFXFM1 to enable islanding of the microgrid.

2.3. Load Curves Modeling

From step 2 onwards, the original (constant) loads of the IEEE model, at PQ buses, were replaced by load curves originated from field measurements [7] (see Figure 2), where the original value of each bus pondered each curve. Three consumer profiles are considered: 1) residential low-income: added in busbars of low-level power; 2) residential middle-income: added in busbars of middle-level power; and 3) commercial: added in busbars of high-level power. All those curves are illustrated in Figure 2. The sampling interval of each curve is 10 minutes. Table I shows the distribution of the load profiles throughout the nodes of the model.

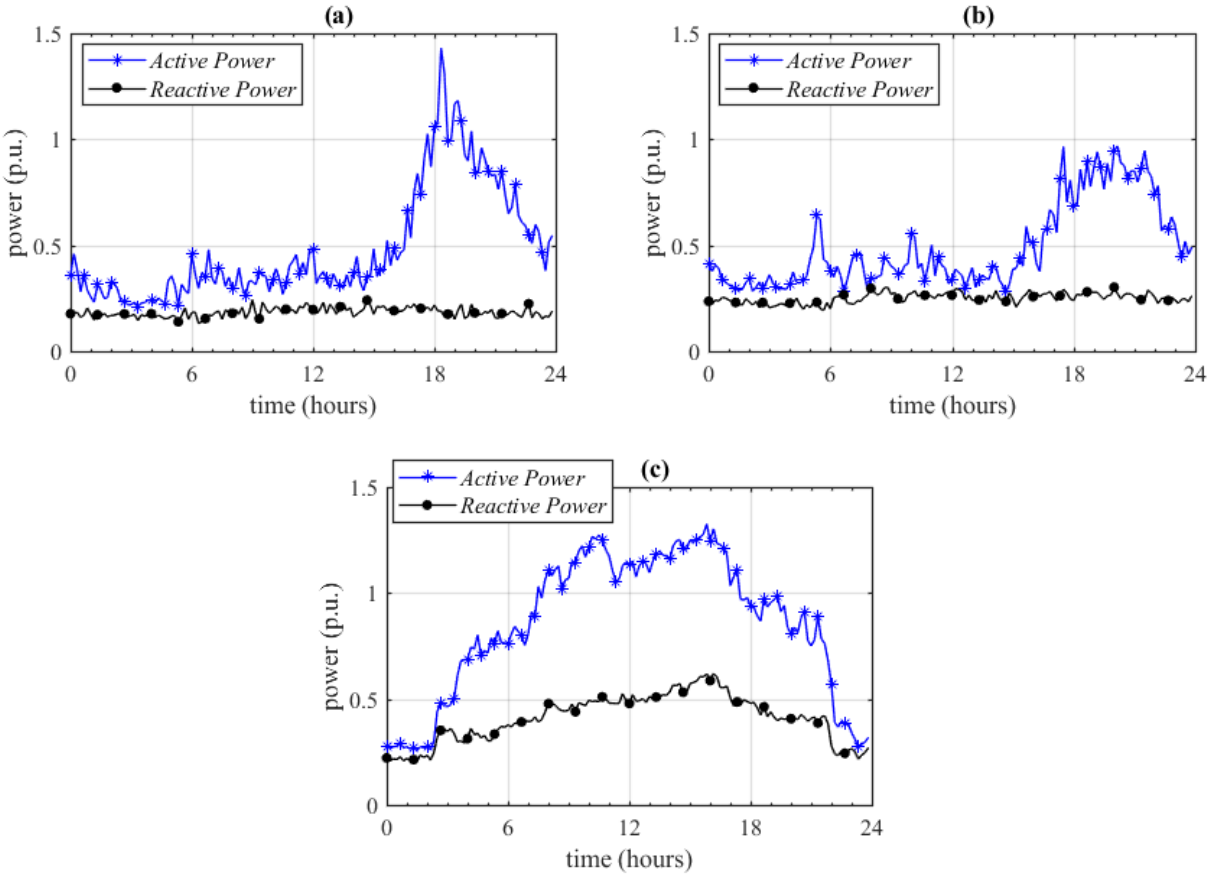

Figure 2: Load curves over a working day for (a) low-income residential, (b) middle-income residential, and (c) commercial profile. Source [7].

Table I: Distribution of the load curves throughout the nodes of the model.

Nodes	Load Profiles
634	Residential low-income
645	Residential low-income
671	Residential middle-income
675	Commercial
632 and 671	Residential low-income

2.4. Photovoltaic Modeling

The photovoltaic system was modeled considering three levels of penetration to investigate the effects of increasing penetration of DG in the distribution system: low (10%), middle (35%), and high (70%) penetration. The definition of penetration level here considered is:

$$Penetration\ Level = \frac{total\ energy\ consumed\ (inside\ MG)\ over\ a\ day}{total\ PV\ energy\ produced\ (inside\ MG)\ over\ a\ day} \times 100\ (\%)$$

In GridLab-D, the PV system was sized and connected to the MG using the Generator Module. The system can be sized by declaring the following characteristics: type (monocrystalline, polycrystalline, amorphous), efficiency, and surface area of the module. In this work, monocrystalline panels with 20% efficiency in the energy conversion were used. The surface area of the PV system (square feet) should be used to define the rated power of the module, which has been sized to suit each of the three penetration level scenarios, as illustrated in Table II. Figure 3 shows the three-phase PV generation curves per penetration level (from GridLab-D). Finally, the inverter connected to the photovoltaic system has been configured with an efficiency of 95% and a mode of operation that provides energy with unit power factor.

Moreover, in a simulation of photovoltaic generation, GridLab-D can consider real meteorological data, such as temperature, solar irradiance, wind, and humidity through the Climate Module. These data can be inserted into the simulation through a file created and supplied by NREL (National Renewable Energy Laboratory). The climate data file used in this work was "WA-Seattle.tmy2" (GridLab-D file sample) that corresponds to the city of Seattle (USA). It is an example commonly used by the GridLab-D developers when modeling IEEE 13 nodes with PV.

Table II: Area versus total energy produced by the PV system for the three penetration levels.

Penetration Level (%)	Area (ft^2)	Total energy produced (kWh)
10	6650	573
35	23275	2006
70	46550	4012

2.5. Battery ESS Modeling

The battery energy storage system was sized and connected to the MG through the Generator

Module, choosing a type (lead-acid or lithium-ion), state of charge (SoC), a round trip efficiency and storage capacity. The simulations were performed with lithium-ion batteries, a round trip of 85% and an initial SoC of 0%. Moreover, the storage capacity of the battery has been dimensioned to allow the storage of all the energy produced by the PV system in each of the scenarios (avoiding consuming power from the main network) and perform its dispatch at peak times. Consequently, each PV penetration level required a different sizing of the battery ESS.

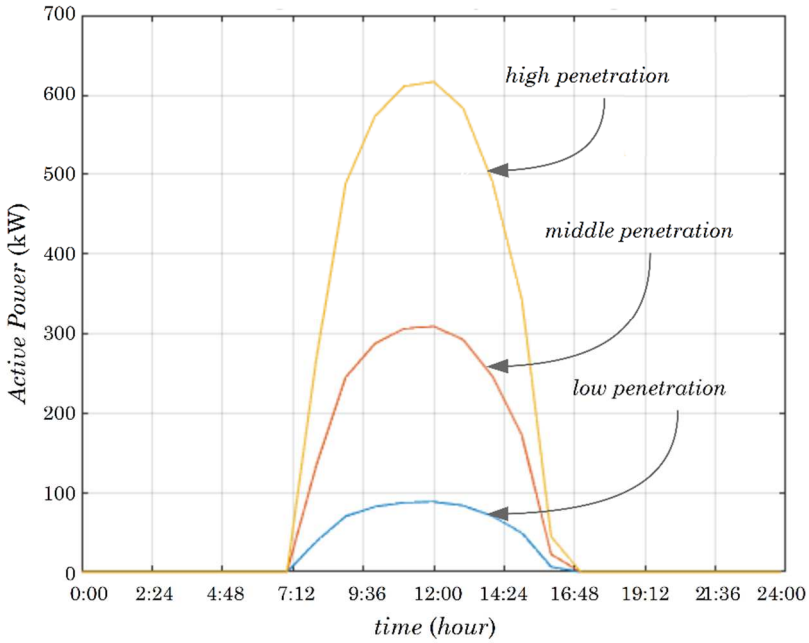

Figure 3: Three-phase PV generation per penetration level (from GridLab-D).

The inverter connected to the battery has been configured to control its power in Load Following mode with monitored power flow on bus 634. Maximum values of charge and discharge rates must also be reported. These parameters can be obtained empirically from the power flow of bus 634. Finally, the inverter connected to the battery ESS has been configured with an efficiency of 95% and a mode of operation that provides energy with unit power factor.

It is emphasized that the program does not support the Load Following mode in the island operation mode. Therefore, to perform such a mode, the Constant PQ mode was used, where the user must create a schedule object, where the values of charging and discharging are specified manually, as well as the instants in which they occur. In this work, the schedule was programmed to store the energy surplus of the PV system and carry out its discharging following the load connected to the microgrid.

2.6. Disconnect Device Modeling

The disconnect device was modeling between the transformer XFXFM1 and bus 634 (see Figure 1). Its opening has been programmed to occur when the production of the PV system is higher than the load demand on the bus 634, to increase the autonomy of the microgrid in the islanded mode.

In the GridLab-D, the activation of the device was performed with the *eventgen* object, contained in the Reliability module, whose purpose is to generate an event at a defined time instant. For the microgrid analysis purposes, it is necessary to include in the simulation the *fault_check* object together with the command line *strictly_radial false*, to indicate to the GridLab-D that there is an island system after an opening event.

When the switch is open, the microgrid loses its swing bus, which initially was the bus 650. Therefore, it is not possible to measure the power flow of the battery and solar generator. However, it is enough to set the bus 634 as a new *SWING_PQ* reference to work around this issue. As far as the authors know, this mode has not yet been documented by the creators of GridLab-D. Consequently, bus 634 is initially configured as *PQ* and becomes a *SWING* at the time of disconnection, thus making simulation in island mode possible. However, to make the *SWING_PQ* mode work, the line *grid_association true* must be added on the *fault_check* object.

3. RESULTS

In step 1, an initial simulation (unbalanced three-phase power flow) was performed considering the IEEE 13 nodes model in its original form for comparison between the values provided with the model (reference values) and the simulated values of this work, to validate both the modeling performed here and the simulators used. In GridLab-D, the results for voltage magnitude showed an average deviation from the reference value of 0.44%, with a maximum value of 0.86% (phase C, bus 611). For the voltage angle, the equivalent values were 0.42% and 3.59% (phase C, RG60). In OpenDSS the results were 1.00%, 1.34% (in phase C, bus 634), 0.41%, and 2.17% (in phase A, bus 634), respectively.

In step 2, the residential and commercial profile load curves were added to the model along with (step 3) the PV generation (bus 634). Figure 4 presents the results of voltage magnitude on bus 634 for phases a, b, and c, considering four scenarios in one day: without PV, with low penetration, middle penetration, and high penetration. This figure shows the voltage rise effect in bus 634 during the period of generation PV (between 7 AM and 5 PM). In the peak generation time (midday), the maximum voltage rise was 0.3%, 1.0%, and 1.9% for the low, middle and high penetration scenarios respectively, all occurring in phase A.

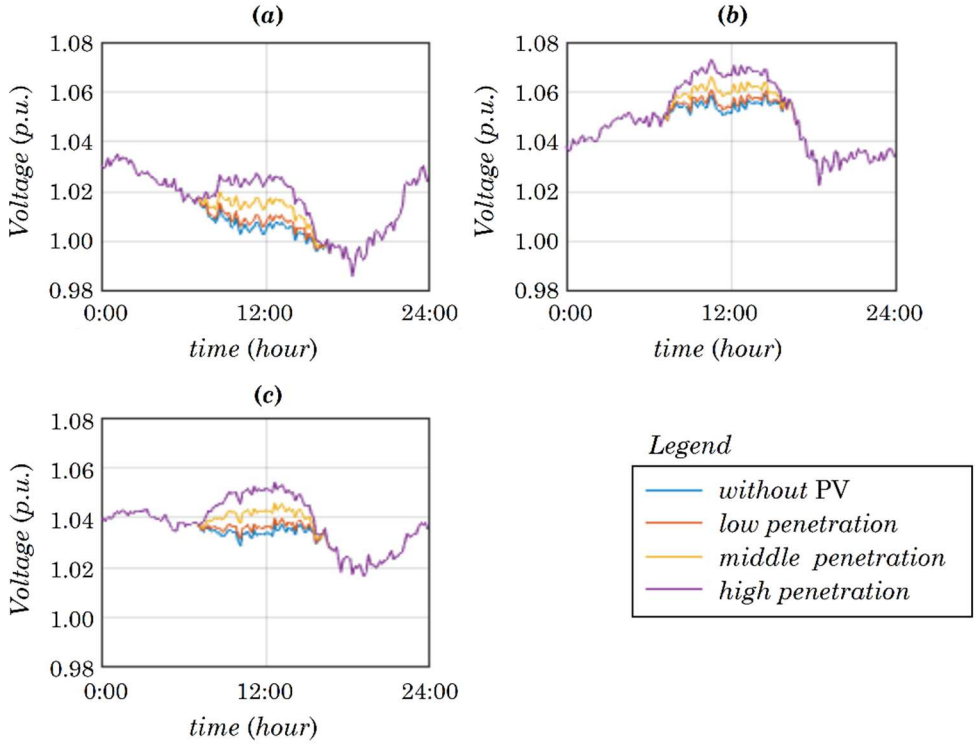

Figure 4: Voltage curves over a day at bus 634 for the four scenarios; (a) phase a; (b) phase b; (c) phase c.

Figure 5(a) shows the power flow on bus 634 over a day to four scenarios: without the insertion of PV, and with low, middle, and high penetrating levels. These results show a negative power flow in the distribution transformer occurring in middle and high penetration scenarios. The latter, at PV peak generation time, causing a reverse power flow of twice the value of the load in the same period. The power flow results, which are illustrated in Figure 5(b) for bus 650, show that the PV insertion into this distribution system has the same effect of a simple negative load block with power values remaining within the usual range of the system.

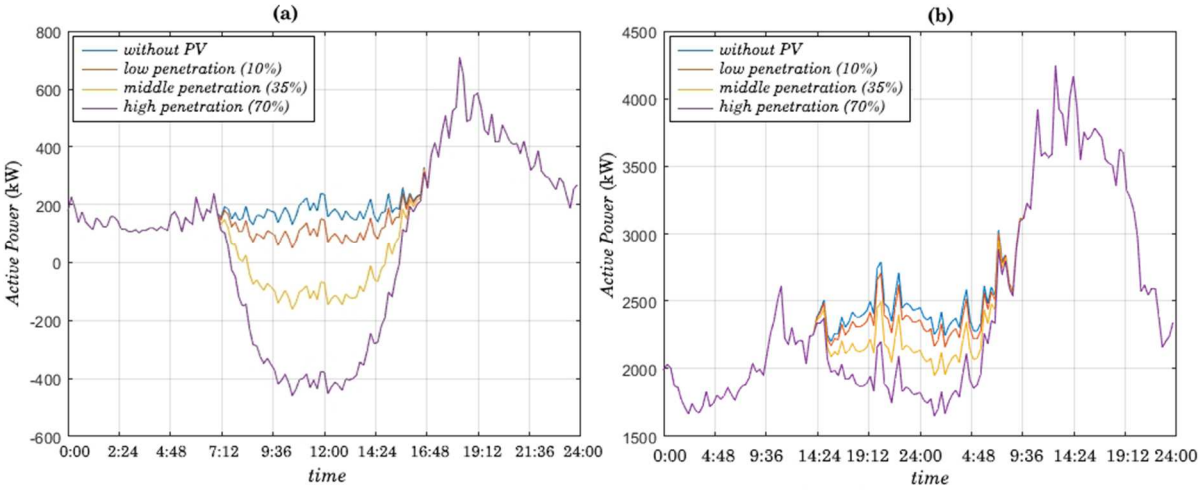

Figure 5: Three-phase power flow for the four penetration cases; (a) bus 634 over a day; (b) bus 650 over two days.

In step 4, the battery ESS was added to the system. The objective of the ESS is to take advantage of the surplus energy in the PV generation period to charge its battery bank and discharge in other periods. Figure 6 shows the results of power flow on bus 634 obtained after ESS insertion (for low, middle, and high penetration). In those three scenarios, the results reveal a flattening in the power curve at the period of peak consumption as an ESS effect. Particularly in the high penetration scenario, it is no longer possible to observe peak consumption. Also, the results show that in all three scenarios, there is no reverse power flow through the distribution transformer. The simulation was done for two days to provide a suitable observation window for the storage system, thus illustrating that there is no accumulation of energy from one day to the next.

Figure 7 illustrates the results obtained for voltage magnitude at bus 634 (phases a, b, and c) after inclusion of the storage system. These results show that with the insertion of the ESS, the effect of voltage rise in that bus was attenuated in all the phases. The scenarios with low, middle and high penetration levels presented a maximum voltage rise of 0.04% 0.57% and 0.60% respectively (at the peak of PV generation), all in phase a.

In step 5, the disconnect switch was added to the simulations to allow the microgrid islanding. The goal is to disconnect the microgrid from the main grid when there is surplus energy (PV generation higher than the microgrid load) and reconnect when the distributed generation (ESS + PV) is no longer enough to meet the load of the microgrid. It was not possible to perform the islanding for the scenario of low penetration of PV because, in this scenario, there is no surplus of generation at any moment.

Table III illustrates a summary of the simulation results for step 5, with four simulation cases. As the autonomy of the microgrid depends on the state of charge of the battery ESS at the moment of

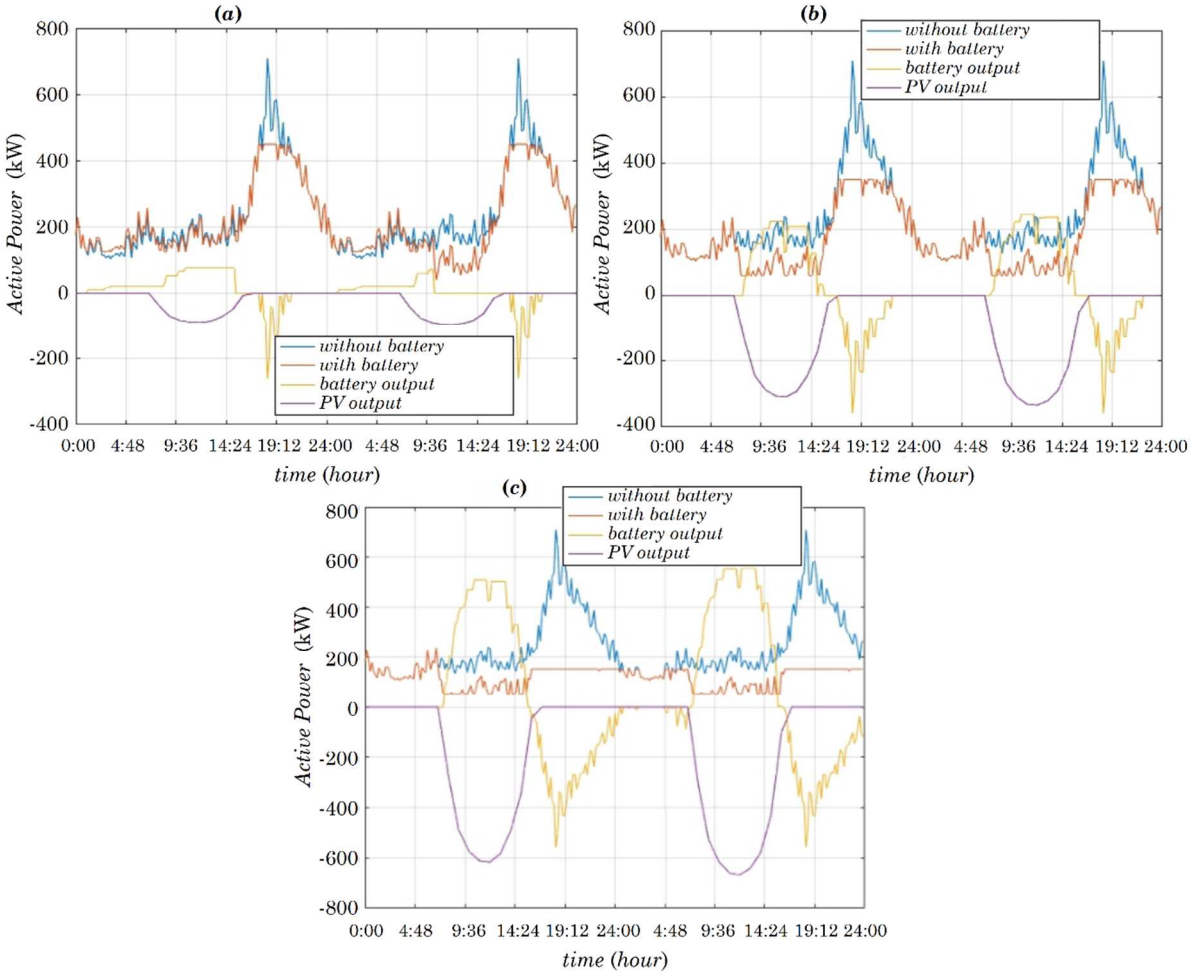

Figure 6: Results of three-phase power flow on bus 634 with battery over two days; (a) low penetration; (b) middle penetration; (c) high penetration.

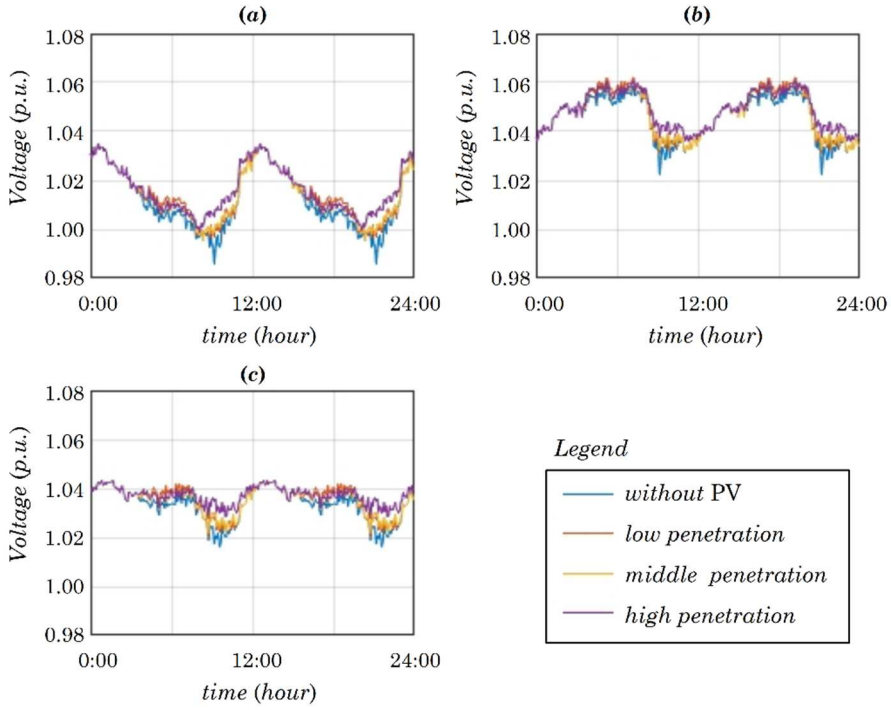

Figure 7: Voltage curves over a day at bus 634 for the four penetration cases and considering battery ESS; (a) phase a; (b) phase b; (c) phase c.

disconnection, then for each level of penetration, two cases were simulated: one for SoC = 0% (cases 1 and 3) and another considering the SoC value that results in the highest possible autonomy (cases 2 and 4). After the islanding event (third column of the table) the loads are fed by the PV generation, and the surplus energy is stored. When the PV generation is no longer enough to support the load of the microgrid, then the dispatch by the battery begins (fourth column of the table). When the battery is no longer able to support the microgrid load, then reconnection to the main grid occurs (fifth column of the table). The microgrid autonomy (sixth column of the table) is calculated from the switch opening event to the end of battery dispatch event. Furthermore, Figure 8 illustrates the impact of the microgrid islanding on the distribution system (bus 650) in middle and high penetration scenarios. At the time of the islanding event, there is a power decrease in bus 650, which for the distribution operator appears to be a loss of load block.

Table III: Microgrid autonomy for four scenarios of penetration and SoC.

Case ID	Scenario [Penetration, SoC]	Switch opening	Start of battery dispatch	End of battery dispatch	Microgrid autonomy
1	[35%, 0%]	08:20	15:00	17:50	9h, 30min
2	[35%, 60%]	08:20	15:00	19:50	11h, 30min
3	[70%, 0%]	07:40	15:40	21:10	13h, 30min
4	[70%, 20%]	07:40	15:40	23:20	15h, 40min

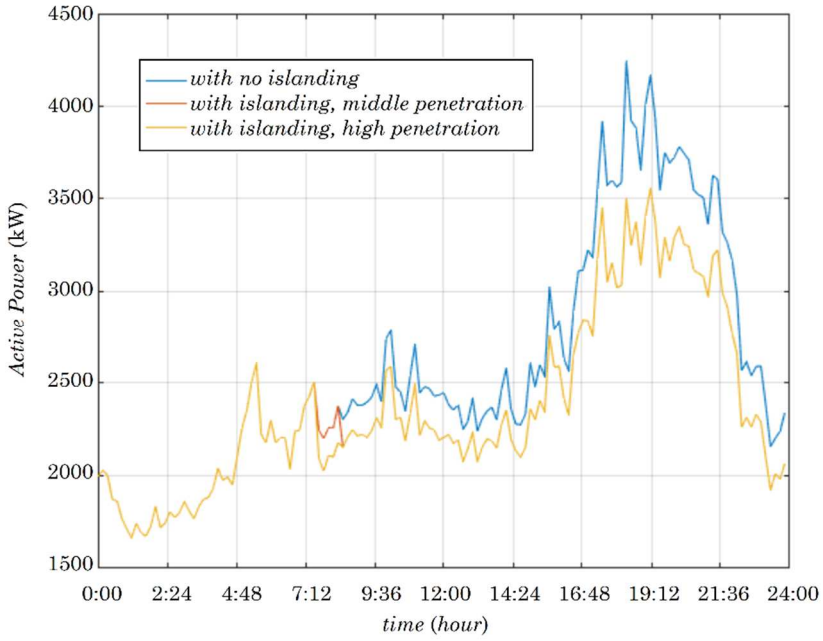

Figure 8: Results for the three-phase power flow over a day, at the bus 650, including the microgrid islanding event.

4. DISCUSSION

Results from step 1 show that there were non-significant deviations from the reference value. Although this difference was smaller in the GridLab-D simulator, both simulators presented similar and numerically equivalent results. These results corroborate to validate both the simulation environment of this work and the two simulators used in the calculation of three-phase unbalanced power flow.

Results from simulations in step2 (Figure 4) show a voltage level increase effect at the low voltage busbar, which is directly proportional to the level of DG penetration. The voltage increase showed a behavior approximately linear with a rate of 0.3% increase in voltage for each 10% increase in the penetration level, reaching around 2% in the high penetration scenario. In practice, such a voltage increase in bus 634 should not be neglected as it may result in a violation of the voltage limits for a low voltage distribution bus. Moreover, in the scenario here analyzed, this effect would occur only during a period (sunshine time), and with intermittent behavior, being more accentuated in the moments of PV generation peak. Thus, it could be a challenge to regulate the voltage at bus 634 because the distribution transformers usually have a fixed tap. Besides, a reverse power flow of more than six hours duration in the distribution transformer was observed (Figure 5(a)) in the 35% and 70% penetration scenarios. On the other hand, the insertion of the PV generation in the bus 634 is not visible from the point of view of the distribution system operator (bus 650), since the power flow results (Figure 5(b)) do not present significant change and can be interpreted as a negative load variation in the system.

In step 4, results (Figure 7) show that the effect of voltage increase on bus 634 can be attenuated with the insertion of a battery ESS on the same bus. All scenarios analyzed showed a reduction in this effect. For example, the increase of local voltage level in high penetration scenario was lower than one-third of that verified previously. Thus, in practice, the ESS significantly mitigates the effects of voltage increase in the microgrid area. Also, results (Figure 6) show that the ESS avoided the reverse power flow in the distribution transformer in all scenarios. It is observed that the battery ESS decreased and flattened the active power flow curve at the distribution transformer in such a way that it was no longer possible to find peak consumption in the high penetration scenario. As a practical consequence, distribution assets (as the distribution transformer) would be relieved at peak times of consumption.

Regarding the island-mode operation (step 5), results show that the autonomy of this microgrid can range from 9 to 15 hours for penetration levels between 35% and 70%. Also, the results show (Figure 8) a systemic load decrease from the viewpoint of DSO, as expected, since the entire load of the microgrid was disconnected from the main grid.

5. CONCLUSIONS

This work shows that both GridLab-D and OpenDSS are suitable tools to calculate three-phase unbalanced power flow, which is essential for carrying out simulations of distribution systems. However, it was identified that only GridLab-D has the option to disconnect the microgrid from the main system during the execution time of simulation, and for this reason, it was adopted as a reference simulator in this work. Then, details on parameterization and modeling of elements such as PV generation, battery ESS, load profile, disconnect device, as well as the adaptation of the IEEE 13 nodes model to support a microgrid busbar, are presented in this work.

Simulation results here presented show some of the relevant impacts of DG, ESS, and microgrids on current power distribution systems, such as the effect of voltage increase on the low voltage bus and the reverse flow in the distribution transformer. On the other hand, it has also been shown that both effects can be attenuated with the insertion of the battery ESS into the microgrid. Besides, with the islanding simulations, it was possible to quantify the autonomy of a microgrid and related it to the penetration levels of PV and the battery ESS sizing.

This work presents the limitation of considering only one microgrid along the distribution feeder. Thus, in future work, simulations with multiple microgrids in the same feeder and at low and middle voltage can be made to investigate their impacts on the distribution system (bus 650) as the effects of penetration level, as well as connection and disconnection of the microgrid.

BIBLIOGRAPHY

[1] M. Jdeed, et al., Smart grid modeling and simulation — Comparing GridLAB-D and RAPSim via two Case studies, (2018 IEEE International Energy Conference (ENERGYCON), Limassol, 2018, pp. 1-6).

[2] M. A. Al Faruque and F. Ahourai., GridMat: Matlab toolbox for GridLAB-D to analyze grid impact and validate residential microgrid level energy management algorithms, (ISGT 2014, Washington, DC, 2014, pp. 1-5).

[3] E. A. F. Nunes, et al., Impact of PV systems on microgrids under different levels of penetration and operational scenarios, (2017 Brazilian Power Electronics Conference (COBEP), Juiz de Fora, 2017, pp. 1-6).

[4] M. A. Mahmud, et al., Analysis of Voltage Rise Effect on Distribution Network with Distributed Generation, (IFAC Proceedings Volumes, volume 44, issue 1, 2011, pp. 14796-14801).

[5] M. A. Zehir, et al., Mitigation of negative impacts of distributed generation on LV distribution networks through microgrid management systems, (2017 IEEE Manchester PowerTech, Manchester, 2017, pp. 1-6).

[6] IEEE Power Engineering Society, IEEE 13 Node Test Feeder, (IEEE, 1992. Available on http://sites.ieee.org/pes-testfeeders/resources/. Accessed in 2017-06-27).

[7] E. K. Yamakawa, Sistema de Controle Nebuloso para Bancos de Capacitores Automáticos Aplicados em Alimentadores de Distribuição de Energia Elétrica (MSc Dissertation. Available on https://acervodigital.ufpr.br/bitstream/handle/1884/14076/Dissertacao%20Final%20Eduardo.pdf?sequence=1 2007).